Nanoscale Advances

ROYAL SOCIETY OF CHEMISTRY

COMMUNICATION

View Article Online
View Journal | View Issue

Cite this: *Nanoscale Adv.*, 2022, **4**, 5253

Received 5th August 2022
Accepted 27th October 2022

DOI: 10.1039/d2na00520d

rsc.li/nanoscale-advances

High-efficiency and simple synthesis of $Ti_3C_2T_x$ nanoscrolls by surface energy modulation and cryogenic freezing†

Ke Tan,‡ Sen Liu,‡ Yang Liu,* Linrui Hou * and Changzhou Yuan *

To alleviate the restacking issue of 2D $Ti_3C_2T_x$ itself, we purposefully explore a simple but efficient method for controllable construction of 1D $Ti_3C_2T_x$ nanoscrolls with a high efficiency of ~90.5%, with detailed regulation of the feed concentrations and surface energy of $Ti_3C_2T_x$. The involved transformation mechanism from 2D nanosheets to 1D nanoscrolls is reasonably proposed.

In recent years, as a new member of two-dimensional (2D) materials, transition metal carbides or carbon/nitride MXenes, with a structure similar to that of graphene, were first reported by Gogotsi in 2011, and afterwards immediately attracted enormous attention worldwide.[1] MXenes are usually prepared by a selective etching-assisted method by removing the A-layer elements (group IIIA or IVA elements, such as Al, Ga, Si or Ge) in the $M_{n+1}AX_n$ (n = 1–3) phase. And the original $M_{n+1}X_nT_x$ (M refers to transition metals and X represents carbon and/or nitrogen) structure can remain unchanged, with –F, –OH and other anion surface functional groups on the surface of nanosheets (NSs) shown as T_x, exhibiting excellent electrical, optical and mechanical properties.[2,3] Compared to traditional 2D materials, MXenes are also endowed with great chemical reactivity and hydrophilicity with functional groups, which is expected to be an ideal matrix material for constructing nanocomposites.[4] Furthermore, the obtained MXene NSs can be exfoliated to monolayer-enriched MXene colloidal solutions towards promising electromagnetic interference shielding and energy storage materials.[5–7] However, mono-layered MXene NSs are always restacked and brought together because of van der Waals interaction and hydrogen bonds, hindering their practical applications because of the poor ion conductivity and electromagnetic wave consumption, which can be solved well by morphology transformation.[8]

The specific morphologies of MXenes play a great role in improving or expanding their properties.[9–12] It has been shown that Ti_2C MXene NSs can be transformed into crumpled sheets, spheres and scrolls by selective intercalation of *p*-phosphonic calix[*n*]arenes, showing new physico-chemical properties.[9] Alkalized MXene nanoribbons with extended interlayer spacing were prepared with excellent Na^+/K^+-storage properties.[10] $Ti_3C_2T_x$ MXene NSs could be scrolled by spray-drying or freeze-drying with Si nanoparticles for electrode materials for Li-ion batteries.[11] Besides, the Ti_3C_2 aerogel synthesized by a simple self-assembly method displays exceptional electrochemical performance for supercapacitors.[12]

Herein, we proposed a highly efficient method to synthesize one-dimensional (1D) $Ti_3C_2T_x$ nanoscrolls through surfactant-assisted lyophilization. Competitively, the formation efficiency of 1D $Ti_3C_2T_x$ nanoscrolls by this way can reach as high as ~90.5% just by optimizing the concentrations of $Ti_3C_2T_x$ NSs dispersion and surfactants. More importantly, with detailed investigations, the essential roles of colloidal solution concentration and surfactants in the scrolling behaviour of $Ti_3C_2T_x$ NSs were rationally put forward.

The $Ti_3C_2T_x$ nanoscrolls were prepared as follows. First, 2.0 g of LiF powder was dissolved in 40 mL of 9 M HCl solution, and stirred for 30 min to prepare etch solution. 2.0 g of Ti_3AlC_2 MAX (11 Technology Co. Ltd.) was added into the solution slowly. After being stirred at 30 °C for 24 h, the suspension was centrifuged at 3500 rpm and washed with deionized (DI) water until the pH value of the solution went up to 6. Second, the obtained precipitate was dispersed into 40 mL of ethyl alcohol and delaminated by sonication under Ar for 1 h. DI water was added after the precipitate was retained in the container by certification. The delaminated $Ti_3C_2T_x$ NSs dispersion can be obtained after being sonicated under Ar for 1 h and centrifuged at 3500 rpm for 5 min, for the formation of a supernatant. The concentration was tested by vacuum drying a certain volume of dispersion at 60 °C for 8 h. Third, 5.0 wt% of surfactants

School of Material Science & Engineering, University of Jinan, Jinan, 250022, P. R. China. E-mail: mse_liuy@ujn.edu.cn; mse_houlr@ujn.edu.cn; mse_yuancz@ujn.edu.cn

† Electronic supplementary information (ESI) available. See DOI: https://doi.org/10.1039/d2na00520d

‡ Ke Tan and Sen Liu equally contributed to the work.

including sodium dodecyl sulfate (SDS), polyvinyl pyrrolidone (PVP) or hexadecyl trimethyl ammonium bromide (CTAB) was dispersed in the diluted $Ti_3C_2T_x$ NSs dispersion of 0.1 g mL^{-1} by stirring at room temperature for 1 h, respectively. Finally, the solutions with SDS, PVP or CTAB were transferred to tubes in liquid N_2 for freezing and drying in freeze-drying equipment for 48 h, and then denoted as $Ti_3C_2T_x$-S, $Ti_3C_2T_x$-P and $Ti_3C_2T_x$-C, respectively. Other $Ti_3C_2T_x$ samples were prepared by the same procedure just with the exception of different concentrations of the $Ti_3C_2T_x$ NSs dispersion and the absence of the surfactant, and named $Ti_3C_2T_x$-n (n = dispersion concentration). $Ti_3C_2T_x$ dispersion (0.1 g mL^{-1}) is directly frozen in a refrigerator (−18 °C), along with the other parameters the same as $Ti_3C_2T_x$-S, and the product was named $Ti_3C_2T_x$-r.

The structures and morphologies of samples were investigated by field-emission scanning electron microscopy (FESEM, JEOL-6300F, 15 kV), transmission electron microscopy (TEM), scanning TEM (STEM), and high-resolution TEM (HRTEM) (JEOL JEM 2100 system) with an energy dispersive X-ray spectroscopy (EDS) system. Crystalline phases were examined using a Rigaku Ultima IV X-ray diffractometer with a Cu Kα radiation source.

The morphologies of $Ti_3C_2T_x$ NSs and $Ti_3C_2T_x$-S were characterized by FESEM and (HR)TEM techniques. Typically, micro-sized $Ti_3C_2T_x$ NSs with transparent features (Fig. 1a and b) and a spacing between layers of ~1.18 nm (Fig. S1†) are evidenced, confirming the successful fabrication of high-quality few-layered $Ti_3C_2T_x$ NSs. It can be visually authenticated by the HRTEM observation (Fig. 1c). One should especially note that some cracked NSs still exist (Fig. 1a) in the freeze-fried $Ti_3C_2T_x$ NSs of original concentration after being frozen by liquid nitrogen. With such a phenomenon in mind, more experiments on feed concentrations are designed later. STEM and corresponding EDX mapping images (Fig. 1d) reveal that there are rich oxygen-containing functional groups on $Ti_3C_2T_x$ NSs. After modification with SDS, rapid freezing by liquid nitrogen and freeze-drying, most $Ti_3C_2T_x$ NSs are rolled up to $Ti_3C_2T_x$-S (Fig. 1e). The diameter of $Ti_3C_2T_x$ nanoscrolls is usually ~200–500 nm, as derived from FESEM and TEM images (Fig. 1f and g). Strikingly, the topological transformation efficiency of $Ti_3C_2T_x$-S is as high as ~90.5%, assessed by counting the number of NSs and nanoscrolls quantitatively in the SEM image (Fig. S2†). The HRTEM image (Fig. 1g) shows that the layer spacing is expanded to ~1.43 nm after rolling-up, corresponding to the low-angle shift tendency of the (002) crystal plane (Fig. S1†), indicating that the addition of SDS and the freezing process further expand the layer spacing. Fig. 1h evidently proves that the nanoscrolls are still $Ti_3C_2T_x$ with oxygen-containing functional groups.

From the discovery of broken $Ti_3C_2T_x$ NSs mentioned before, the sheets dispersion is diluted to successively decreasing concentrations and freeze-dried directly after freezing with liquid N_2 without SDS. The morphologies of these samples with different concentrations ranging from 2.0 to 0.1 g mL^{-1} (Fig. 2a–f) visualize that more $Ti_3C_2T_x$ NSs can be scrolled up and more broken NSs appear as the concentration decreases. Specifically, $Ti_3C_2T_x$-2.0 (Fig. 2a) still presents a sheet-shape structure, and $Ti_3C_2T_x$-1.0 (Fig. 2b) is partly broken. As the concentration decreases, most NSs of $Ti_3C_2T_x$-0.8 (Fig. 2c) are broken and nanoscrolls start to appear in $Ti_3C_2T_x$-0.5 (Fig. 2d). More and more nanoscrolls are discerned with further decreasing the concentration of $Ti_3C_2T_x$ dispersion, particularly for the case of $Ti_3C_2T_x$-0.1 (Fig. 2f). Note that the NSs start to roll up inward from the edge closer to freshly formed ice in $Ti_3C_2T_x$-0.8, while the NSs in $Ti_3C_2T_x$-0.2 and $Ti_3C_2T_x$-0.1 are half/full rolling up with a lower rolling degree than $Ti_3C_2T_x$-S. Their digital pictures (the insets in Fig. 2) show that the volume of $Ti_3C_2T_x$ in the form of aerogels gets smaller and smaller as the dispersion concentration decreases. It can be rationally attributed to the larger size of $Ti_3C_2T_x$ NSs and the too fast growth rate of ice crystals by liquid N_2 freezing. When the concentration is reduced to a certain extent, the rapidly growing ice crystals tear the NSs apart into smaller sizes as they cannot hinder them, as revealed by the schematic illustration (Fig. S3†).

As mentioned above, $Ti_3C_2T_x$ NSs modified with the anion surfactant of SDS can be well rolled-up after freezing by liquid N_2 and freezing-drying. To better understand the phenomenon, two other surfactants (*i.e.*, cationic CTAB and non-ionic PVP) are

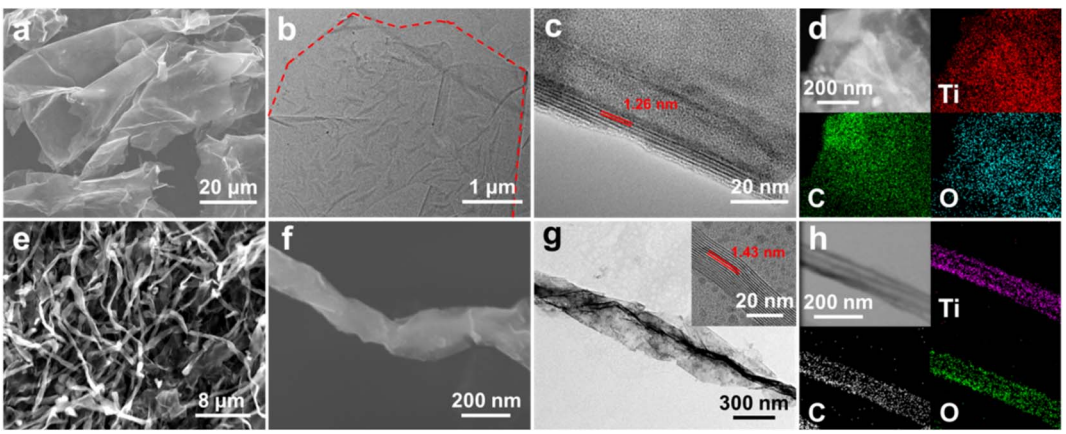

Fig. 1 (a) FESEM, (b) TEM, (c) HRTEM, and (d) STEM and corresponding EDX mapping images of $Ti_3C_2T_x$ NSs; (e and f) FESEM, (g) TEM and HRTEM (the inset in panel (g)), and (h) STEM and corresponding EDX mapping images of $Ti_3C_2T_x$-S.

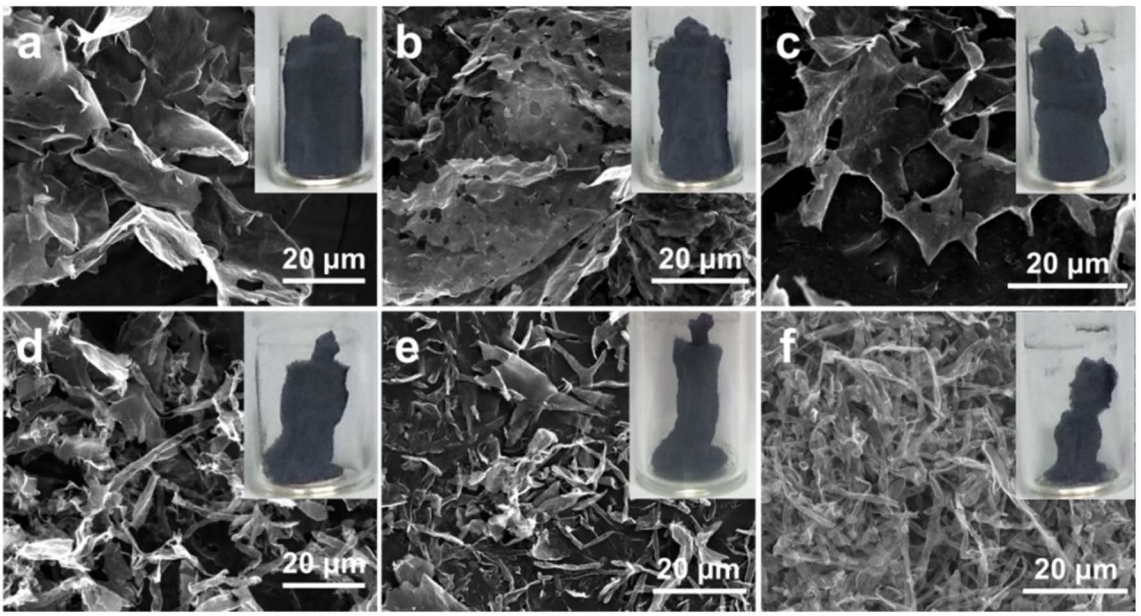

Fig. 2 FESEM images and digital pictures (the insets) of (a) $Ti_3C_2T_x$-2.0, (b) $Ti_3C_2T_x$-1.0, (c) $Ti_3C_2T_x$-0.8, (d) $Ti_3C_2T_x$-0.5, (e) $Ti_3C_2T_x$-0.2 and (f) $Ti_3C_2T_x$-0.1 samples.

evaluated as well like SDS with $Ti_3C_2T_x$ NSs, and their morphological transformation results are shown in Fig. 3a–d. Interestingly, for the case of $Ti_3C_2T_x$-C, most of the $Ti_3C_2T_x$ NSs are still flat and half-rolled up sheets, along with merely a small number of nanoscrolls (Fig. 3a and b). In contrast, $Ti_3C_2T_x$-P (Fig. 3c and d) consists of half-rolled up NSs and nanoscrolls, about half of each. The distinct difference among the three cases should be related to the different natures of the three surfactants. Generally, the anionic surfactant of SDS further can enhance the electronegativity of the NSs with original anion surface functional groups (–F and –OH), while a cationic surfactant or non-ionic surfactant could reduce the electronegativity and enhance the stability of $Ti_3C_2T_x$ NSs. When the temperature drops rapidly, $Ti_3C_2T_x$ NSs tend to roll up and shrink to reduce surface energy. And more pronounced the tendency to roll up becomes, the greater the electronegativity.

For figuring out the influence of the dropping rate of freezing temperature, $Ti_3C_2T_x$ NSs are frozen under ~−18 °C in a refrigerator for comparison. Clearly, the integral NSs even larger than ~50 μm in size are obvious for $Ti_3C_2T_x$-r (Fig. 3e and

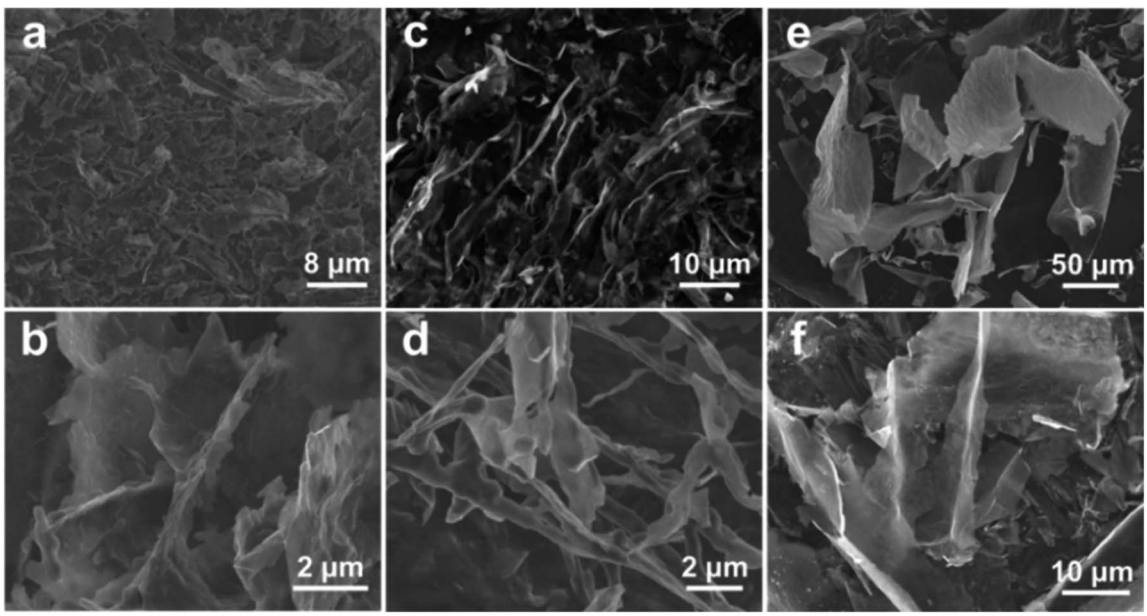

Fig. 3 FESEM images of (a and b) $Ti_3C_2T_x$-C and (c and d) $Ti_3C_2T_x$-P frozen with liquid N_2, and (e and f) $Ti_3C_2T_x$-r.

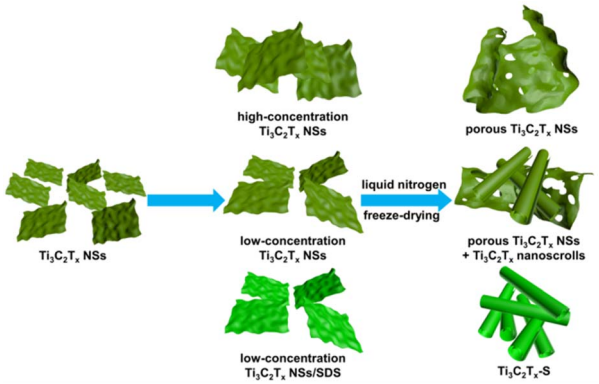

Fig. 4 Schematic illustration for synthesizing different $Ti_3C_2T_x$ structures through regulation of concentrations and electronegativity.

f), which is not broken by ice crystals. This can be attributed to ice crystals that just grow along the NSs when the temperature is dropped slowly and the stress work on the NSs is too small to break and/or squeeze them much (Fig. S4†). This can be used for the delamination of MXenes, as reported in detail before.[13]

Combining the above phenomenon of different concentrations and surfactant modifications, the morphological transformations of $Ti_3C_2T_x$ NSs themselves manifest in different forms, as schematically summarized in Fig. 4. When the concentration is relatively high, the stress generated by the growth of ice crystals can only break the $Ti_3C_2T_x$ NSs and rolling-up of them cannot be achieved because of their mutual obstacles. As regards the relatively low concentration, some of the broken $Ti_3C_2T_x$ NSs roll up for lower surface energy to accommodate the super low environment, so the porous NSs and nanoscrolls co-exist in the case. After being modified with SDS, nearly all $Ti_3C_2T_x$ NSs roll up when frozen with liquid nitrogen as they are more unstable. As for $Ti_3C_2T_x$-S, some structures in the intermediate state show how broken $Ti_3C_2T_x$ NSs rolled up (Fig. S5a and b†). When the ice crystal punctures $Ti_3C_2T_x$ NSs, a temperature difference in a localized area containing ice and broken NSs is created temporarily. The ambient temperature at the edge of the NSs near the ice is much higher than that at the other part farther away from the ice, so the NSs are rolled up from this edge for a more stable state. The interconnected types of nanoscrolls show a typical scrolling morphology containing trunk-to-trunk and head-to-trunk structures (Fig. S5c–f†). Commonly, the trunk-to-trunk structure is formed by crossing mutually independent NSs, and the head-to-trunk structure is formed from the same NSs.

Conclusions

In summary, a highly efficient and simple method was devised to controllably synthesize 1D $Ti_3C_2T_x$ nanoscrolls by surface energy modulation and cryogenic freezing. The formation of 1D $Ti_3C_2T_x$ nanoscrolls was rationally proposed with detailed morphological and structural characteristics. Benefitting from the enhanced electronegativity by an anionic surfactant and the fast freezing rate of liquid nitrogen, $Ti_3C_2T_x$ NSs were spontaneously rolled up to keep stable as they are in the area of temporary temperature imbalance. More meaningfully, our contribution here will provide a functional building block to construct 1D versatile $Ti_3C_2T_x$ nanoscroll based composites, hugely promoting comprehensive research and applications of $Ti_3C_2T_x$ MXenes in energy storage, electromagnetic interference shielding, catalytic conversion, and beyond.

Conflicts of interest

There are no conflicts to declare.

Acknowledgements

The authors acknowledge the financial support from the National Natural Science Foundation of China (No. 52072151, 52171211, 5210021292, and 52271218) and Taishan Scholars (No. ts201712050).

References

1 M. Naguib, M. Kurtoglu, V. Presser, J. Lu, J. J. Niu, M. Heon, L. Hultman, Y. Gogotsi and M. W. Barsoum, *Adv. Mater.*, 2011, **23**, 4248–4253.
2 M. Naguib, V. N. Mochalin, M. W. Barsoum and Y. Gogotsi, *Adv. Mater.*, 2014, **26**, 992–1005.
3 C. J. Lu, L. Yang, B. Z. Yan, L. B. Sun, P. G. Zhang, W. Zhang and Z. M. Sun, *Adv. Funct. Mater.*, 2020, **30**, 2000852.
4 H. C. Huang, H. Su, H. T. Zhang, L. D. Xu, X. Chu, C. F. Hu, H. Liu, N. J. Chen, F. Y. Liu, W. Deng, B. N. Gu, H. P. Zhang and W. Q. Yang, *Adv. Electron. Mater.*, 2018, **4**, 1800179.
5 Q. W. Wang, H. B. Zhang, J. Liu, S. Zhao, X. Xie, L. X. Liu, R. Yang, N. Koratkar and Z. Z. Yu, *Adv. Funct. Mater.*, 2018, **29**, 1806819.
6 W. Z. Bao, L. Liu, C. Y. Wang, S. Choi, D. Wang and G. X. Wang, *Adv. Energy Mater.*, 2018, **8**, 1702485.
7 M. Z. Yu, Z. Y. Wang, J. S. Liu, F. Sun, P. J. Yang and J. S. Qiu, *Nano Energy*, 2019, **63**, 103880.
8 K. Li, M. Y. Liang, H. Wang, X. H. Wang, Y. S. Huang, J. Coelho, S. Pinilla, Y. L. Zhang, F. W. Qi, V. Nicolosi and Y. X. Xu, *Adv. Funct. Mater.*, 2020, **30**, 2000842.
9 A. Vaughn, J. Ball, T. Heil, D. J. Morgan, G. I. Lampronti, G. Maršalkaitė, C. L. Raston, N. P. Power and S. Kellici, *Chem.–Eur. J.*, 2017, **23**, 8128–8133.
10 P. C. Lian, Y. F. Dong, Z. S. Wu, S. H. Zheng, X. H. Wang, S. Wang, C. L. Sun, J. Q. Qin, X. Y. Shi and X. H. Bao, *Nano Energy*, 2017, **40**, 1–8.
11 J. N. Meng, F. F. Zhang, L. Zhang, L. Y. Liu, J. T. Chen, B. J. Yang and X. B. Yan, *J. Energy Chem.*, 2020, **46**, 256–263.
12 L. Li, M. Y. Zhang, X. T. Zhang and Z. G. Zhang, *J. Power Sources*, 2017, **364**, 234–241.
13 X. W. Huang and P. Y. Wu, *Adv. Funct. Mater.*, 2020, **30**, 1910048.